Tests of hadronic vacuum polarization fits for the muon anomalous magnetic moment

Maarten Golterman,[1,2] Kim Maltman,[3,4] and Santiago Peris[5]

[1]*Institut de Física d'Altes Energies (IFAE), Universitat Autònoma de Barcelona, E-08193 Bellaterra, Barcelona, Spain*
[2]*Department of Physics and Astronomy, San Francisco State University, San Francisco, California 94132, USA*
[3]*Department of Mathematics and Statistics, York University, Toronto, Ontario, Canada M3J 1P3*
[4]*CSSM, University of Adelaide, Adelaide, South Australia 5005, Australia*
[5]*Department of Physics, Universitat Autònoma de Barcelona, E-08193 Bellaterra, Barcelona, Spain*

(Received 18 September 2013; published 9 December 2013)

Using experimental spectral data for hadronic τ decays from the OPAL experiment, supplemented by a phenomenologically successful parametrization for the high-s region not covered by the data, we construct a physically constrained model of the isospin-one vector-channel polarization function. Having such a model as a function of Euclidean momentum Q^2 allows us to explore the systematic error associated with fits to the Q^2 dependence of lattice data for the hadronic electromagnetic current polarization function which have been used in attempts to compute the leading order hadronic contribution, $a_\mu^{\rm HLO}$, to the muon anomalous magnetic moment. In contrast to recent claims made in the literature, we find that a final error in this quantity of the order of a few percent does not appear possible with current lattice data, given the present lack of precision in the determination of the vacuum polarization at low Q^2. We also find that fits to the vacuum polarization using fit functions based on vector meson dominance are unreliable, in that the fit error on $a_\mu^{\rm HLO}$ is typically much smaller than the difference between the value obtained from the fit and the exact model value. The use of a sequence of Padé approximants known to converge to the true vacuum polarization appears to represent a more promising approach.

DOI: 10.1103/PhysRevD.88.114508 PACS numbers: 12.38.Gc, 12.38.−t, 13.40.Gp

I. INTRODUCTION

In the quest for a precision computation of the muon anomalous magnetic moment $a_\mu = (g-2)/2$, the contribution from the hadronic vacuum polarization at lowest order in the fine-structure constant α, $a_\mu^{\rm HLO}$, plays an important role. While the contribution itself is rather small (of order 0.06 per mille) the error in this contribution dominates the total uncertainty in the present estimate of the Standard Model value. In order to reduce this uncertainty, and resolve or solidify the potential discrepancy between the experimental and Standard Model values, it is thus important to corroborate, and if possible improve on, the total error in $a_\mu^{\rm HLO}$.

Recently, there has been much interest in computing this quantity using lattice QCD [1]. In terms of the vacuum polarization $\Pi^{\rm em}(Q^2)$ at Euclidean momenta Q^2, $a_\mu^{\rm HLO}$ is given by the integral [2,3]

$$
\begin{aligned}
a_\mu^{\rm HLO} &= 4\alpha^2 \int_0^\infty dQ^2 f(Q^2)(\Pi^{\rm em}(0) - \Pi^{\rm em}(Q^2)), \\
f(Q^2) &= m_\mu^2 Q^2 Z^3(Q^2) \frac{1 - Q^2 Z(Q^2)}{1 + m_\mu^2 Q^2 Z^2(Q^2)}, \\
Z(Q^2) &= \left(\sqrt{(Q^2)^2 + 4m_\mu^2 Q^2} - Q^2\right)/(2m_\mu^2 Q^2),
\end{aligned}
\tag{1.1}
$$

where m_μ is the muon mass, and for nonzero momenta $\Pi^{\rm em}(Q^2)$ is defined from the hadronic contribution to the electromagnetic vacuum polarization $\Pi^{\rm em}_{\mu\nu}(Q)$,

$$
\Pi^{\rm em}_{\mu\nu}(Q) = (Q^2\delta_{\mu\nu} - Q_\mu Q_\nu)\Pi^{\rm em}(Q^2) \tag{1.2}
$$

in momentum space.

Since the integral is over Euclidean momentum, this is an ideal task for the lattice, if $\Pi^{\rm em}(Q^2)$ can be computed at sufficiently many nonzero values of Q^2, especially in the region $Q^2 \sim m_\mu^2$ which dominates the integral. However, because of the necessity of working in a finite volume, momenta are quantized on the lattice, which turns out to make this a difficult problem. Figure 1 demonstrates the problem. On the left, we see a typical form of the subtracted vacuum polarization, together with the low-Q^2 points from a typical lattice data set.[1] On the right, we see the same information, but now multiplied by the weight $f(Q^2)$ in Eq. (1.1).

Figure 1 clearly shows why evaluating the integral in Eq. (1.1) as a Riemann sum using typical lattice data is ruled out. In principle, going to larger volumes or using twisted boundary conditions [4,5] can help, but it will be necessary to fit the lattice data for $\Pi(Q^2)$ to a continuous function of Q^2 in order to evaluate the integral. The problem then becomes that of finding a theoretically well-founded functional form for the Q^2 dependence of $\Pi(Q^2)$, so that this functional form can be fitted to available data, after which the integral in Eq. (1.1) is performed using the fitted function.

A number of fit functions have been used and/or proposed recently. One class of fit functions is based on vector

[1]For the curve and data shown here, see Secs. II and IV.

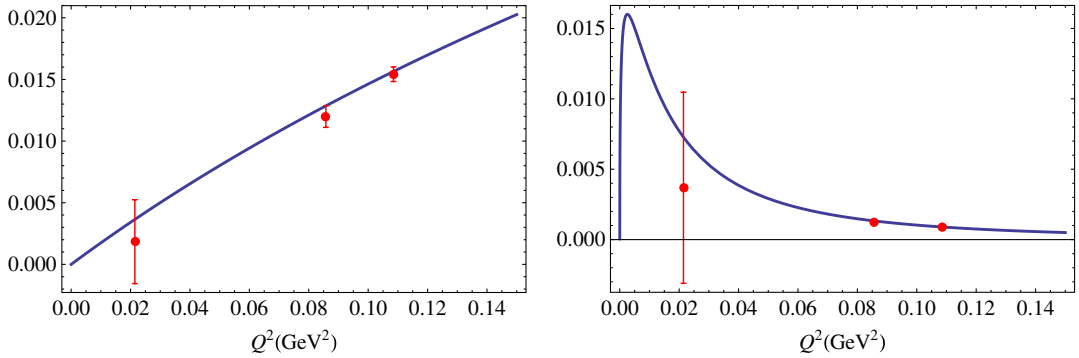

FIG. 1 (color online). Low-Q^2 behavior of the subtracted vacuum polarization $\Pi(0) - \Pi(Q^2)$ (left panel) and of the integrand $f(Q^2)(\Pi(0) - \Pi(Q^2))$ in Eq. (1.1) (right panel). Red points show typical data on a $64^3 \times 144$ lattice with lattice spacing 0.06 fm and periodic boundary conditions.

meson dominance (VMD) [6–8], another class on Padé approximants (PAs) [4,9], while a position-space version of VMD-type fits was recently proposed in Ref. [10]. VMD-type fits, as well as the PAs used in Ref. [4], do not represent members of a sequence of functions guaranteed to converge to the actual vacuum polarization, whereas the PAs of Ref. [9] do. Thus, theoretical prejudice would lead one to choose the PAs of Ref. [9] as the appropriate set of functions to fit lattice data for the vacuum polarization.

However, this does not guarantee that any particular fit to lattice data for the vacuum polarization will yield an accurate estimate of $a_\mu^{\rm HLO}$ with a reliable error. This depends not only on the theoretical validity of the fit function, but also, simply, on the availability of good data. Moreover, even if a sequence of PAs converges (on a certain Q^2 interval), not much is known in practice about how fast its rate of convergence may be. For example, if the convergence is very slow given a certain lattice data set, it could be that only PAs with a number of parameters far beyond the reach of these data give a numerically adequate representation of the true vacuum polarization, for the goal of computing $a_\mu^{\rm HLO}$ to a phenomenologically interesting accuracy.

It would therefore be useful to have a good model, in which the "exact" answer is known. One can then investigate any given fitting method, and ask questions such as whether a good fit (for instance, as measured by the χ^2 per degree of freedom) leads to an accurate result for $a_\mu^{\rm HLO}$. If the model is a good model, this will not only test the theoretical validity of a given fit function, but also how well this fit works, given a required accuracy, and given a set of data for $\Pi(Q^2)$. In other words, it will give us a reliable quantitative estimate of the systematic error.

Such a model is available for the vacuum polarization. The $I = 1$ nonstrange hadronic vector spectral function has been very accurately measured in hadronic τ decays. From this spectral function, one can, using a dispersion relation, construct the corresponding component of the vacuum polarization, if one has a reliable theoretical representation for the spectral function beyond the τ mass. Such a representation was constructed in Refs. [11,12] from OPAL data for this spectral function [13]. The thus obtained vacuum polarization is closely related to the $I = 1$ component of the vacuum polarization obtained from $\sigma(e^+e^- \to \gamma \to$ hadrons).

Three points are relevant to understanding the use of the term "model" for the resulting $I = 1$ polarization function, in the context of the underlying $a_\mu^{\rm HLO}$ problem. First, $a_\mu^{\rm HLO}$ is related directly to $\sigma(e^+e^- \to \gamma \to$ hadrons) [14] and the associated electromagnetic (EM) current polarization function, which, unlike the model, has both an $I = 1$ and $I = 0$ component. Second, even for the $I = 1$ part there are subtleties involved in relating the spectral functions obtained from $\sigma(e^+e^- \to \gamma \to$ hadrons) and nonstrange τ decays [15,16]. Finally, since the τ data extend only up to $s = m_\tau^2$, a model representation is required for the $I = 1$ spectral function beyond this point.

In fact, we consider the pure $I = 1$ nature of the model polarization function an advantage for the purposes of this study, as it corresponds to a simpler spectral distribution than that of the EM current (the latter involving also the light quark and $\bar{s}s$ $I = 0$ components). Working with the τ data also allows us to avoid having to deal with the discrepancies between the determinations of the $\pi^+\pi^-$ electroproduction cross sections obtained by different experiments [17–20].[2] We should add that, though a model is needed for the part of the $I = 1$ spectral function beyond $s = m_\tau^2$, for the low-Q^2 values relevant to $a_\mu^{\rm HLO}$, the vacuum polarization we construct is very insensitive to the parametrization used in this region. Finally, we note that the model vacuum polarization satisfies, by construction, the same analyticity properties as the real vacuum polarization. In particular, the subtracted model vacuum polarization is equal to Q^2 times a Stieltjes function [9]. We thus expect our model to be an excellent model for the purpose

[2]Figures 48 and 50 of Ref. [19] provide a useful overview of the current situation.

of this article, which is to test a number of methods that have been employed in fitting the Q^2 dependence of the vacuum polarization to lattice data, and not to determine the $I = 1$ component of $a_\mu^{\rm HLO}$ from τ spectral data.

This article is organized as follows. In the following two sections, we construct the model and define the fit functions we will consider here. Throughout this paper, we will consider only VMD-type fits, which have been extensively used, and PA fits of the type defined in Ref. [9].[3] In Sec. IV, we use the model and a typical covariance matrix obtained in a lattice computation to generate fake "lattice" data sets, which are then fitted in Sec. V. We consider both correlated and diagonal ("uncorrelated") fits, where in the latter case errors are computed by linear propagation of the full data covariance matrix through the fit. From these fits, estimates for $a_\mu^{\rm HLO}$ with errors are obtained, and compared with the exact model value in order to test the accuracy of the fits. Section VI contains our conclusions.

II. CONSTRUCTION OF THE MODEL

The nonstrange, $I = 1$ subtracted vacuum polarization is given by the dispersive integral

$$\tilde{\Pi}(Q^2) = \Pi(Q^2) - \Pi(0) = -Q^2 \int_{4m_\pi^2}^{\infty} dt \frac{\rho(t)}{t(t+Q^2)}, \tag{2.1}$$

where $\rho(t)$ is the corresponding spectral function, and m_π the pion mass. In order to construct our model for $\tilde{\Pi}(Q^2)$, we split this integral into two parts: one with $4m_\pi^2 \le t \le s_{\rm min} \le m_\tau^2$, and one with $s_{\rm min} \le t < \infty$. In the first region, we use OPAL data to estimate the integral by a simple Riemann sum:

$$(\Pi(Q^2) - \Pi(0))_{t \le s_{\rm min}} = -Q^2 \Delta t \sum_{i=1}^{N_{\rm min}} \frac{\rho(t_i)}{t_i(t_i+Q^2)}. \tag{2.2}$$

Here the t_i label the midpoints of the bins from the lowest bin $i = 1$ to the highest bin $N_{\rm min}$ below $s_{\rm min} = N_{\rm min}\Delta t$, and Δt is the bin width, which for the OPAL data we use is equal to 0.032 GeV^2. For the contribution from the spectral function above $s_{\rm min}$, we use the representation

$$(\Pi(Q^2) - \Pi(0))_{t \ge s_{\rm min}} = -Q^2 \int_{s_{\rm min}}^{\infty} dt \frac{\rho_{t \ge s_{\rm min}}(t)}{t(t+Q^2)}, \tag{2.3a}$$

$$\rho_{t \ge s_{\rm min}}(t) = \rho_{\rm pert}(t) + e^{-\delta-\gamma t}\sin(\alpha+\beta t), \tag{2.3b}$$

where $\rho_{\rm pert}(t)$ is the perturbative part calculated to five loops in perturbation theory, expressed in terms of $\alpha_s(m_\tau^2)$ [21], with m_τ the τ mass. The oscillatory term is our representation of the duality-violating part, and models

[3]For other PA fits considered in the literature, we are not aware of any convergence theorems.

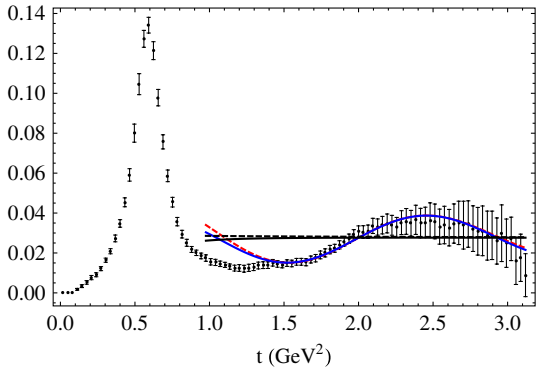

FIG. 2 (color online). The $I = 1$ nonstrange vector spectral function, from Ref. [12], as a function of t. The data are from OPAL [13]; the curves are theoretical representations obtained from the $w = 1$ finite-energy sum rule discussed in Refs. [11,12].

the presence of resonances in the measured spectral function. This representation of the spectral function was extensively investigated in Refs. [11,12], and found to give a very good description of the data between $s_{\rm min} = 1.504$ GeV^2 and m_τ^2. Figure 2 shows the comparison between the data and the representation (2.3b) for this value of $s_{\rm min}$; the blue continuous curve shows the representation we will be employing here. Our central values for $\alpha_s(m_\tau^2)$, α, β, γ and δ have been taken from the FOPT $w = 1$ finite-energy sum rule fit of Ref. [12][4]:

$$\begin{aligned} &\alpha_s(m_\tau^2) = 0.3234, \\ &\alpha = -0.4848, \qquad \beta = 3.379\ \text{GeV}^{-2}, \\ &\gamma = 0.1170\ \text{GeV}^{-2}, \qquad \delta = 4.210. \end{aligned} \tag{2.4}$$

The low-Q^2 part of the function $\Pi(Q^2)$ obtained through this strategy is shown as the blue curve in the left-hand panel of Fig. 1.

As in Ref. [9] we will take as a benchmark the low- and medium-Q^2 part of $a_\mu^{\rm HLO}$,

$$\tilde{a}_\mu^{{\rm HLO},Q^2\le 1} = 4\alpha^2 \int_0^{1\ \text{GeV}^2} dQ^2 f(Q^2)(\Pi(0) - \Pi(Q^2)). \tag{2.5}$$

To make it clear that we are computing this quantity from $\tilde{\Pi}(Q^2)$ defined from Eqs. (2.1)–(2.4), and not from $\Pi^{\rm em}(Q^2)$, we will use the symbol $\tilde{a}_\mu$, instead of a_μ, in the rest of this article.

Using the OPAL data as described above, and fully propagating errors,[5] we find the value

[4]The final one or two digits of these parameter values are not significant in view of the errors obtained in Eq. (5.3) of Ref. [12], but these are the values we used to construct the model.

[5]Taking into account the OPAL data covariance matrix, the parameter covariance matrix for the parameters in Eq. (2.3b), as well as the correlations between OPAL data and the parameters.

$$\tilde{a}_\mu^{\mathrm{HLO},Q^2\le 1} = 1.204(27)\times 10^{-7}. \tag{2.6}$$

In our tests of lattice data in Sec. V below, we will declare the model to be "exact," and see how various fits to fake lattice data generated from the model will fare in reproducing this exact value. For our purposes, it is sufficient to have a four-digit "exact" value, which we take to be

$$\tilde{a}_{\mu,\mathrm{model}}^{\mathrm{HLO},Q^2\le 1} = 1.204\times 10^{-7}. \tag{2.7}$$

We close this section with a few remarks. In the region $0 \le Q^2 \le 1$ GeV^2, the model we constructed for $\tilde{\Pi}(Q^2)$ is very insensitive to both the detailed quantitative form of Eq. (2.3b), as well as to the choice of $s_{\min}$. Moreover, the precise quantitative values that we obtain for $\tilde{\Pi}(Q^2)$ as a function of Q^2 are not important. What is important is that this is a very realistic model, based on hadronic data which are very well understood in the framework of QCD, for the $I = 1$ part of $\Pi^{\mathrm{em}}(Q^2)$.

III. FIT FUNCTIONS

We will consider two classes of fit functions to be employed in fits to data for $\Pi(Q^2)$. The first class of functions involves PAs of the form

$$\Pi(Q^2) = \Pi(0) - Q^2\left(a_0 + \sum_{k=1}^{K}\frac{a_k}{b_k + Q^2}\right). \tag{3.1}$$

For $a_0 = 0$, the expression between parentheses is a $[K-1, K]$ Padé; if also a_0 is a parameter, it is a $[K, K]$ Padé. With $a_{k\ge 1} > 0$ and $b_k > b_{k-1} > \cdots > b_1 > 4m_\pi^2$, these PAs constitute a sequence converging to the exact vacuum polarization in the sense described in detail in Ref. [9]. With "good enough" data, we thus expect that, after fitting the data, one or more of these PAs will provide a numerically accurate representation of $\Pi(Q^2)$ on a compact interval for Q^2 on the positive real axis. For each such fit, we may compute $\tilde{a}_\mu^{\mathrm{HLO},Q^2\le 1}$, and compare the result to the exact model value. Of course, the aim of this article is to gain quantitative insight into what it means for the data to be "good enough," as well as into what order of PA might be required to achieve a given desired accuracy in the representation of $\Pi(Q^2)$ at low Q^2.

We note that in the model, by construction we have that $\tilde{\Pi}(0) = 0$. In contrast, a lattice computation yields only the unsubtracted $\Pi(Q^2)$ at nonzero values of Q^2.[6] It thus appears that the model does not quite match the lattice framework it is designed to simulate. However, if in the test fits we treat $\Pi(0)$ in Eq. (3.1) as a free parameter, we discard the information that $\tilde{\Pi}(0) = 0$ in the model, and we can use the fake data generated from the model as a test case for the lattice. In other words, if we treat $\Pi(0)$ in Eq. (3.1) as a free parameter, we can think of the model vacuum polarization as $\Pi(Q^2)$ in a scheme in which $\Pi(0)$ happens to vanish, rather than as $\tilde{\Pi}(Q^2)$. This turns out to be a very important observation, because even if a PA- or VMD-type fit does a good job of fitting the overall Q^2 behavior over a given interval, it is generally difficult for these fits to yield the correct curvature at very low Q^2. Because the integral in Eq. (1.1) is dominated by the low-Q^2 region, this effect can lead to significant deviations of $\tilde{a}_\mu^{\mathrm{HLO},Q^2\le 1}$ from the exact model value, as we will see below.

We will also consider VMD-type fits, which have been widely used in the literature. Typical VMD-type fits have the form of Eq. (3.1), but with the lowest pole, b_1, fixed to the ρ mass, $b_1 = m_\rho^2$. We will consider two versions: straight VMD, obtained by taking $K = 1$ in Eq. (3.1) and setting $a_0 = 0$, and VMD +, which is similar but with a_0 a free parameter. Such VMD-type fits have been employed previously [4,6–8,24]. We emphasize that VMD-type fits, despite their resemblance to the PAs of Eq. (3.1), are *not* of that type. The exact function $\Pi(Q^2)$ has a cut at $Q^2 = -4m_\pi^2$, which has to be reproduced by the gradual accumulation of poles in Eq. (3.1) toward that value. If instead we choose the lowest pole at the ρ mass, the fit function is a model function based on the intuitive picture of vector meson dominance, and is definitely not a member of the convergent sequence introduced in Ref. [9]. However, as already emphasized in Sec. I, the aim here is to investigate the quality of various fits on test data, without theoretical prejudice. We will thus investigate both PA- and VMD-type fits in the remainder of this article.

In Ref. [8] also a VMD-type fit with two poles, obtained by choosing $K = 2$, $a_0 = 0$ and $b_1 = m_\rho^2$, has been considered. In our case, such a fit turns out not to yield any extra information beyond VMD +: we always find that b_2 is very large, and a_2 and b_2 are very strongly correlated, with the value of a_2/b_2 equal to the value of a_0 found in the VMD+ fit. The reason this does not happen in Ref. [8] is probably that in that case also the connected part of the $I = 0$ component is included in $\Pi(Q^2)$, and this component has a resonance corresponding to the octet component of the ϕ-ω meson pair. In our case, in which only the $I = 1$ component is present, these two-pole VMD-type fits never yield any information beyond the VMD+ fits.

IV. THE GENERATION OF FAKE LATTICE DATA

In order to carry out the tests, we need data that correspond to a world described by our model, and that resemble a typical set of lattice data. In order to construct such a data

[6] A recent paper proposed a method for computing $\Pi(0)$ directly on the lattice [22], whereas another recent paper proposed a method to obtain $\Pi(Q^2)$ at and near $Q^2 = 0$ by analytic continuation [23]. Since we do not know yet what the size of the combined statistical and systematic errors on $\Pi(0)$ determined in such ways will turn out to be, we do not consider these options in this article.

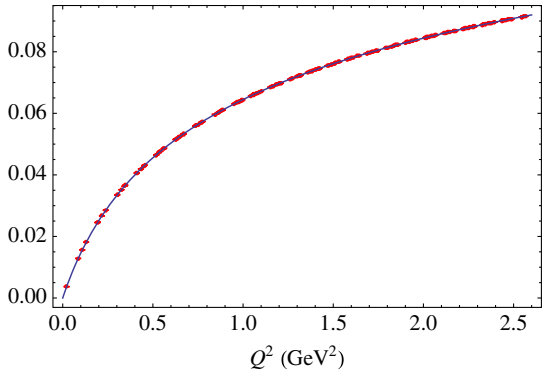

FIG. 3 (color online). Fake data set constructed in Sec. IV and the model for $\Pi(0) - \Pi(Q^2)$ constructed in Sec. II (thin blue curve).

set, we proceed as follows. First, we choose a set of Q^2 values. The Q^2 values we will consider are those available on an $L^3 \times T = 64^3 \times 144$ lattice with periodic boundary conditions, and an inverse lattice spacing $1/a = 3.3554$ GeV. The smallest momenta on such a lattice in the temporal and spatial directions are

$$Q = \left(0, 0, 0, \frac{2\pi}{aT}\right) \rightarrow Q_1^2 = 0.02143 \text{ GeV}^2,$$
$$Q = \left(0, 0, 0, \frac{4\pi}{aT}\right) \rightarrow Q_2^2 = 0.08574 \text{ GeV}^2, \quad (4.1)$$
$$Q = \left(\frac{2\pi}{aL}, 0, 0, 0\right) \rightarrow Q_3^2 = 0.1085 \text{ GeV}^2,$$

etc. Next, we construct a multivariate Gaussian distribution with central values $\Pi(Q_i^2)$, $i = 1, 2, \ldots$, and a typical covariance matrix obtained in an actual lattice computation of the vacuum polarization on this lattice. The covariance matrix we employed is the covariance matrix for the $a = 0.06$ fm data set considered in Ref. [9]. The fake data set is then constructed by drawing a random sample from this distribution.[7] The data points shown in Fig. 1 are the first three data points of this fake data set. The full data set is shown in Fig. 3. We will refer to this as the "lattice" data set.

Below, we will also have use for a "science fiction" data set. This second data set is obtained exactly as the fake data set described above, except that we first divide the lattice covariance matrix by 10000, which corresponds to reducing diagonal errors by a factor 100. After this reduction, the data set is generated as before. We refer to this as the science-fiction data set because it seems unlikely that a realistic lattice data set with such good statistics will exist in the near future. However, this second data set will allow us to gain some additional insights in the context of this model study.

[7]We used the Mathematica routines MultinormalDistribution and RandomVariate.

V. FITS TO THE FAKE LATTICE DATA

In this section, we will present and discuss the results of a number of fits, based on the data sets constructed in Sec. IV.

A. Lattice data set

Table I shows the results of a number of correlated fits of the lattice data set to the functional forms defined in Sec. III. To the left of the vertical double line the fitted data are those in the interval $0 < Q^2 \leq 1$ GeV^2; to the right the fitted data are those in the interval $0 < Q^2 \leq 1.5$ GeV^2. In each of these two halves, the leftmost column shows the fit function, and the second column gives the value of $\tilde{a}_\mu^{\text{HLO},Q^2\leq 1}$ obtained from the fit, with the χ^2 fit error between parentheses. The "pull" σ in the third column is defined as

$$\sigma = \frac{|\text{exact value} - \text{fit value}|}{\text{error}}. \quad (5.1)$$

For instance, with the exact value of Eq. (2.7), we have for the [1, 1] PA on the interval $0 < Q^2 \leq 1$ GeV^2 that $\sigma = |1.204 - 1.116|/0.022 = 4$. The fourth column gives the χ^2 value per degree of freedom (d.o.f.) of the fit.

Of course, the pull can only be computed because we know the exact model value. This is precisely the merit of this model study: it gives us insight into the quality of the fit independent of the χ^2 value. Clearly, the fit does a good job if the pull is of order 1, because if that is the case, the fit error covers the difference between the exact value and the fitted value.

The primary measure of the quality of the fit is the value of χ^2/d.o.f. This value clearly rules out [0, 1] PA and VMD as good fits. In this case, we do not even consider the pull: these functional forms clearly just do not represent the data very well. However, in all other cases, one might consider the value of χ^2/d.o.f. to be reasonable, although less so for fits on the interval $0 < Q^2 \leq 1.5$ GeV^2. However, only the [1, 2] and [2, 2] PAs have a good value for the pull for fits on the interval $0 < Q^2 \leq 1$ GeV^2, whereas the pull for the [1, 1] PA and VMD+ is bad: the fit error does not nearly cover the difference between the true (i.e., exact model) value and the fitted value. Note that with the errors of the lattice data set even the best result, from the [2, 2] PA, only reaches an accuracy of 5% for $\tilde{a}_\mu$. On the interval $0 < Q^2 \leq 1.5$ GeV^2 all fits get worse, both as measured by χ^2 and σ, and only the [2, 2] PA may be considered acceptable.

For illustration, we show the [1, 2] PA and VMD+ fits on the interval $0 < Q^2 \leq 1$ GeV^2 in Figs. 4 and 5. The left-hand panels show the fit over a wider range of Q^2, including the full set of Q^2 values employed in the fit, while the right-hand panels focus on the low-Q^2 region of the integrand in Eq. (1.1) of primary relevance to $\tilde{a}_\mu^{\text{HLO},Q^2\leq 1}$, which contains only a few of the Q^2 fit points. The blue solid

TABLE I. Various correlated fits of the lattice data set constructed in Sec. IV on the interval $0 < Q^2 \leq 1$ GeV^2 (left of the vertical double line), or on the interval $0 < Q^2 \leq 1.5$ GeV^2 (right of the vertical double line). For a more detailed description, see the text.

Fit	$\tilde{a}_\mu^{\mathrm{HLO},Q^2\leq 1} \times 10^7$	σ	χ^2/d.o.f.	$\tilde{a}_\mu^{\mathrm{HLO},Q^2\leq 1} \times 10^7$	σ	χ^2/d.o.f.
PA [0, 1]	0.8703(95)		285/46	0.6805(45)		1627/84
PA [1, 1]	1.116(22)	4	61.4/45	1.016(12)	16	189/83
PA [1, 2]	1.182(43)	0.5	55.0/44	1.117(22)	4	129/82
PA [2, 2]	1.177(58)	0.5	54.6/43	1.136(38)	1.8	128/81
VMD	1.3201(52)		2189/47	1.3873(44)		18094/85
VMD+	1.0658(76)	18	67.4/46	1.1041(48)	21	243/84

curve shows the exact model, the green dashed curve the fit, and the red points are the lattice data. Both fits to the vacuum polarization look like good fits (confirmed by the χ^2/d.o.f. values) when viewed from the perspective of the left-hand panels. A clear distinction, however, emerges between the [1, 2] PA and VMD+ cases when one focuses on the low-Q^2 region shown in the right-hand panels. In these panels, the PA fit follows the exact curve very closely, while the VMD+ fit undershoots the exact curve by a significant amount, as quantified by the pull. Looking at the left-hand panels in Figs. 4 and 5, one would never suspect the difference in the results for $\tilde{a}_\mu^{\mathrm{HLO},Q^2\leq 1}$ illustrated in the corresponding right-hand panels.

B. Science-fiction data set

In Table II, we show the same type of fits as in Table I, but now using the science-fiction data set defined in Sec. IV. The corresponding figures are very similar to Figs. 4 and 5, and hence are not shown here.

This data set is, of course, quite unrealistic: real lattice data with such precision will not soon be generated. But

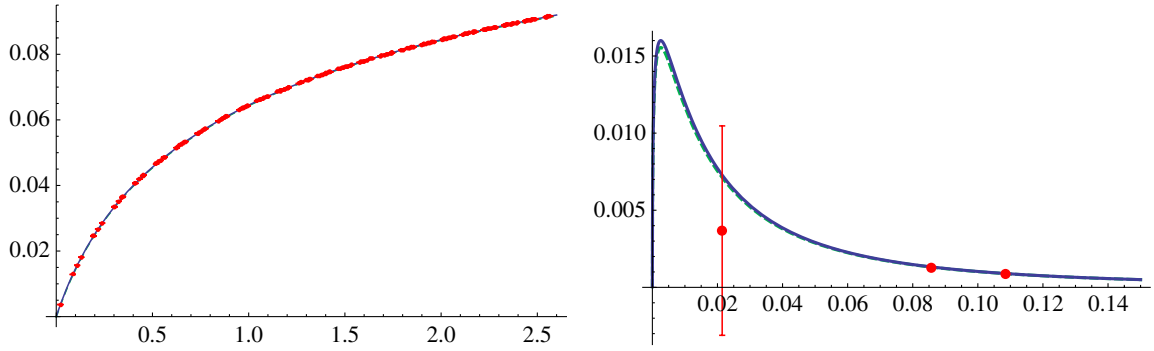

FIG. 4 (color online). The [1, 2] PA fit on the interval $0 < Q^2 \leq 1$ GeV^2 of Table I: green dashed curves, in comparison with the model (blue solid curves). The left panel shows the vacuum polarization and the right panel shows the blown-up low-Q^2 region of the integrand of Eq. (1.1); red points are lattice data points. Axes and units are as in Fig. 1.

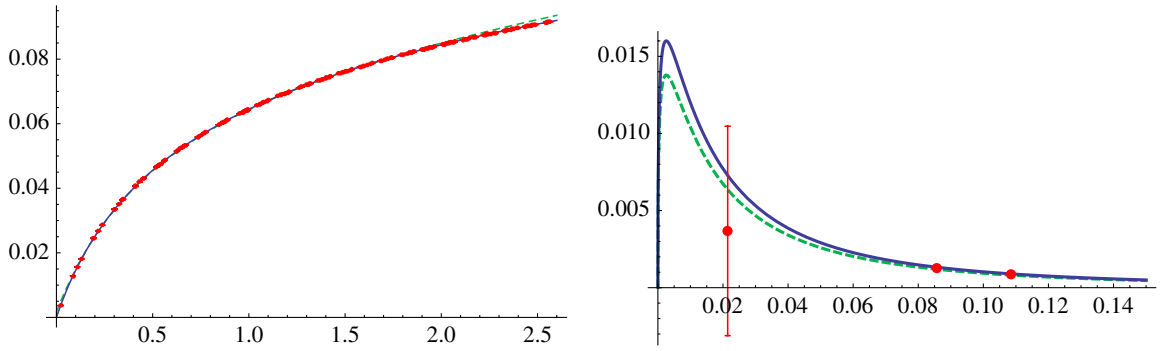

FIG. 5 (color online). The VMD+ fit on the interval $0 < Q^2 \leq 1$ GeV^2 of Table I: green dashed curves, in comparison with the model (blue solid curves). The left panel shows the vacuum polarization and the right panel shows the blown-up low-Q^2 region of the integrand of Eq. (1.1); red points are lattice data points. Axes and units are as in Fig. 1.

TABLE II. Fits analogous to those reported in Table I, obtained using the science-fiction data set, for which the covariance matrix was reduced by a factor 10000. The fitting interval is $0 < Q^2 \leq 1$ GeV^2.

Fit	$\tilde{a}_\mu^{\mathrm{HLO},Q^2\leq 1} \times 10^7$	σ	χ^2/d.o.f.
PA [0, 1]	0.87782(9)		1926084/46
PA [1, 1]	1.0991(2)		51431/45
PA [1, 2]	1.1623(4)		1340/44
PA [2, 2]	1.1862(15)	12	76.4/43
PA [2, 2]	1.1965(28)	2	42.0/42
VMD	1.31861(5)		20157120/47
VMD+	1.07117(8)		70770/46

these fits address the question of which of the fit functions considered might still be acceptable in this hypothetical world, and whether simply decreasing the errors, in this case by the large factor of 100, rather than also filling in low-Q^2 values, will be sufficient to achieve the goal of getting to the desired $\sim$1% accuracy in the determination of $\tilde{a}_\mu^{\mathrm{HLO},Q^2\leq 1}$. The answer is barely.

First, we see that the VMD-type fits are completely ruled out already by the χ^2 values. The higher precision data are also more punishing on the PA fits. By χ^2 values, the first three PAs are excluded, in contrast to Table I, where only the [0, 1] PA is really excluded by its χ^2 value. The [2, 2] PA has a possibly reasonable χ^2 value, but its accuracy does not match its precision, with a pull equal to 12.[8] The more precise data make it possible to perform a [2, 3] PA fit, and this fit is borderline acceptable, given the value of the pull.

The best fit for each data set yields $a_\mu^{\mathrm{HLO},Q^2\leq 1}$ with an error of 5% for the lattice data set, down to 0.2% for the science-fiction data set. While this means that (real) lattice data with a precision somewhere in between would yield an error of order 1% or below, we also see from this example that that precision does not necessarily translate into an equal accuracy. We conjecture that in order to increase accuracy, data at more low-Q^2 values than present in the fake data sets considered here will be needed. While precision data in the region of the peak of the integrand would be ideal, we suspect that filling in the region between the two lowest Q^2 values in this data set might already be of significant help.

C. Diagonal fits

It is important to emphasize that the data sets considered here are constructed such that by definition the covariance matrix employed is the true covariance matrix, and not some estimator for the true one. However, it is possible that for some unknown reason the covariance matrix we employed for generating the fake data set is less realistic, even though we took it to come from an actual lattice computation. For instance, the vacuum polarization of this lattice computation contains both $I = 1$ and (the connected part of the) $I = 0$ components, whereas the vacuum polarization considered here has only an $I = 1$ component.

For this reason, we also considered diagonal fits, in which instead of minimizing the χ^2 function, we minimize the quadratic form $\mathcal{Q}^2$ obtained by keeping only the diagonal of the covariance matrix. However, our errors take into account the full data covariance matrix by linear error propagation. (For a detailed description of the procedure, see the appendix of Ref. [11].[9])

TABLE III. Fits like those reported in Table I, but using a diagonal fit quality $\mathcal{Q}^2$, and linear propagation of errors. Fitting interval $0 < Q^2 \leq 1$ GeV^2 (left of the vertical double line), or $0 < Q^2 \leq 1.5$ GeV^2 (right of the vertical double line).

	$\tilde{a}_\mu^{\mathrm{HLO},Q^2\leq 1} \times 10^7$	σ	$\mathcal{Q}^2$	$\tilde{a}_\mu^{\mathrm{HLO},Q^2\leq 1} \times 10^7$	σ	$\mathcal{Q}^2$
PA [0, 1]	0.997(23)	19	20.1	0.906(15)	20	62.4
PA [1, 1]	1.173(74)	0.4	13.8	1.108(39)	2.5	30.3
PA [1, 2]	1.30(32)	0.3	13.55	1.22(15)	0.1	29.5
VMD	1.2122(82)	1	75.2	1.2895(69)	12	510
VMD+	1.083(17)	7	15.0	1.081(12)	10	30.7

TABLE IV. Diagonal fits like those reported in Table III, but using the science-fiction data set. Fitting interval $0 < Q^2 \leq 1$ GeV^2.

	$\tilde{a}_\mu^{\mathrm{HLO},Q^2\leq 1} \times 10^7$	σ	$\mathcal{Q}^2$
PA [0, 1]	0.99623(23)		40350
PA [1, 1]	1.12875(68)		623
PA [1, 2]	1.1762(21)	13	31.3
PA [2, 2]	1.1904(54)	2.5	22.1
VMD	1.21076(8)		589751
VMD+	1.08341(16)		4081

Results of diagonal fits are shown in Tables III and IV. These tables show fits analogous to those shown in Tables I and II, but instead of taking the full covariance matrix into account through a χ^2 fit, it is only taken into account in the error propagation, after the fit parameters have been determined from a diagonal fit.

The results of these diagonal fits are consistent with, and confirm, the conclusions one draws from the correlated fits shown in Tables I and II. For PA fits, the only differences are that errors from the diagonal fits are larger, and the maximum order of the PA for which we can find a stable fit is one notch lower. Since the fit quality $\mathcal{Q}^2$ is not a χ^2

[8]We define the "precision" as the error we obtain, while the "accuracy" is the difference between the exact and fitted values.

[9]We prefer to refer to this type of fit as a "diagonal" fit, instead of an "uncorrelated" fit, as the latter phrase suggests, incorrectly, that the off-diagonal part of the covariance matrix is completely omitted from the analysis.

function, its absolute value (per degree of freedom) has no quantitative probabilistic meaning. But clearly the [0, 1], [1, 1], VMD and VMD+ fits shown in Table IV are bad fits, as judged from their $\mathcal{Q}^2$ values. We therefore did not compute the pull for these fits. For all other fits in Tables III and IV the pull is shown and is consistent' with those shown in Tables I and II for PAs of one higher order.

Also from these diagonal fits we conclude that the VMD-type fits considered here do not work. Amusingly, VMD appears to get it right, if one takes the VMD fit on the interval $0 < Q^2 \leq 1$ GeV^2 in Table III at face value. However, this should be considered an accident. If one adds a parameter to move to a VMD+ fit, the value of $\mathcal{Q}^2$ decreases significantly, as it should, but the pull increases dramatically, showing that VMD+ is not a reliable fit. This should not happen if the VMD result were to be reliable itself. Likewise, if we change the fitting interval from $0 < Q^2 \leq 1$ GeV^2 to $0 < Q^2 \leq 1.5$ GeV^2, the pull increases much more dramatically than for the PA fits. In addition, both VMD-type fits in Table IV are bad fits, as judged by the $\mathcal{Q}^2$ values, even though, because of the same accident, the VMD value for $a_\mu^{\mathrm{HLO},Q^2\leq 1}$ looks very good. Note, however, that again the error is nowhere near realistic as well: we did not compute the pull because of the large $\mathcal{Q}^2$ value, but its value given the numbers reported is very large.

We conclude from this example that in order to gauge the reliability of a fit, ideally one should consider a sequence of fit functions in which parameters are systematically added to the fit function. This allows one to test the stability of such a sequence of fits, and avoid mistakenly interpreting an accidental agreement with the model result as an indication that a particular fit strategy is reliable when it is not, as happens here for the VMD fit and the specific 0 to 1 GeV^2 fitting window. The PA approach provides a systematic sequence of fit functions in this respect.

D. The region $1 \leq Q^2 \leq 2$ GeV^2

While higher-order PAs appear to work reasonably well, in the sense that their accuracy matches their precision, we also noted that on our fake lattice data set this is less true when one increases the fit interval from $0 < Q^2 \leq 1$ GeV^2 to $0 < Q^2 \leq 1.5$ GeV^2. At the same time, one expects QCD perturbation theory only to be reliable above approximately 2 GeV^2. This leads to the question whether one can do better on the interval between 0 and 2 GeV^2.

As we saw in Sec. V, the accuracy of the contribution to $\tilde{a}_\mu^{\mathrm{HLO},Q^2\leq 1}$ is limited to about 5% on the lattice data set, because of the relatively sparse data at low values of Q^2. We will therefore limit ourselves here to a few exploratory comments, in anticipation of future data sets with smaller errors in the low-Q^2 region, and a denser set of Q^2 values.[10]

A possible strategy is to fit the data using a higher-order PA on the interval $0 < Q^2 \leq Q^2_{\mathrm{max}}$, while computing the contribution between Q^2_{max} and 2 GeV^2, $\tilde{a}_\mu^{\mathrm{HLO},Q^2_{\mathrm{max}}\leq Q^2\leq 2}$, directly from the data, for some value of Q^2_{max} such that the PA fits lead to reliable results for $\tilde{a}_\mu^{\mathrm{HLO}}$ on the interval between 0 and Q^2_{max}. This is best explained by an example, in which we choose $Q^2_{\mathrm{max}} \approx 1$ GeV^2.

The Q^2 value closest to 1 GeV^2 is $Q^2_{49} = 0.995985$ GeV^2; that closest to 2 GeV^2 is $Q^2_{129} = 2.00909$ GeV^2. From our fake data set, using the covariance matrix with which it was generated, we use the trapezoidal rule to find an estimate

$$\begin{aligned}\tilde{a}_\mu^{\mathrm{HLO},Q^2_{49}\leq Q^2\leq Q^2_{129}} &= \frac{1}{2}\sum_{i=49}^{128}(Q^2_{i+1}-Q^2_i)(f(Q^2_i)(\Pi(0)-\Pi(Q^2_i)) \\ &\quad + f(Q^2_{i+1})(\Pi(0)-\Pi(Q^2_{i+1}))) \\ &= 6.925(26)\times 10^{-10} \quad \text{(estimate)}. \end{aligned} \tag{5.2}$$

This is in good agreement with the exact value

$$\tilde{a}_\mu^{\mathrm{HLO},0.995985\leq Q^2\leq 2.00909} = 6.922\times 10^{-10} \quad \text{(exact)}. \tag{5.3}$$

On this interval no extrapolation in Q^2 is needed, nor does the function $f(Q^2)$ play a "magnifying" role, so we expect the error in Eq. (5.2) to be reliable, and we see that this is indeed the case. In contrast, it is obvious from Fig. 1 that estimating $\tilde{a}_\mu^{\mathrm{HLO},Q^2\leq 1}$ in this way would not work. One may now combine the estimate (5.2) with, for instance, the result from a fit to the [1, 2] PA on the interval $0 < Q^2 \leq 0.995985$ GeV^2 in order to estimate $\tilde{a}_\mu^{\mathrm{HLO},Q^2\leq 2.00909}$.[11] The error on this estimate would be determined completely by that on $\tilde{a}_\mu^{\mathrm{HLO},Q^2\leq 1}$ coming from the fit, since the error in Eq. (5.2) is tiny. Of course, in a complete analysis of this type, correlations between the "fit" and "data" parts of $\tilde{a}_\mu^{\mathrm{HLO}}$ should be taken into account, because the values obtained for the fit parameters in Eq. (3.1) will be correlated with the data. However, we do not expect this to change the basic observation of this subsection: the contribution to $\tilde{a}_\mu^{\mathrm{HLO}}$ from the Q^2 region between 1 and 2 GeV^2 can be estimated directly from the data with a negligible error, simply because this contribution to $\tilde{a}_\mu^{\mathrm{HLO}}$ is itself very small (less than 0.6%). With better data, this strategy can be optimized by varying the value of Q^2_{max}.

VI. CONCLUSION

In order to compute the lowest-order hadronic vacuum polarization contribution a_μ^{HLO} to the muon anomalous magnetic moment, it is necessary to extrapolate lattice

[10] A denser set can be obtained by going to larger volumes, and/or the use of twisted boundary conditions [4,5].

[11] The result from this fit is identical to that on the interval $0 < Q^2 \leq 1$ GeV^2 given in Table I to the precision shown in that table.

data for the hadronic vacuum polarization $\Pi(Q^2)$ to low Q^2. Because of the sensitivity of $a_\mu^{\rm HLO}$ to $\Pi(Q^2)$ in the Q^2 region around m_μ^2, one expects a strong dependence on the functional form used in order to fit data for $\Pi(Q^2)$ as a function of Q^2.

It is therefore important to test various possible forms of the fit function, and a good way to do this is to use a model. Given a model, given a set of values of Q^2 at which lattice data are available, and given a covariance matrix typical of the lattice data, one can generate fake data sets, and test fitting methods by comparing the difference between the fitted and model values for $a_\mu^{\rm HLO}$ with the error on the fitted value obtained from the fit. In this article, we carried out such tests, using a model constructed from the OPAL data for the $I = 1$ hadronic spectral function as measured in τ decays, considering fit functions based on both vector meson dominance and a sequence of Padé approximants introduced in Ref. [9]. We took our Q^2 values and covariance matrix from a recent lattice data set with lattice spacing 0.06 fm and volume $64^3 \times 144$ [9].

For a fake data set generated for these Q^2 values with the given covariance matrix, we found that indeed it can happen that the precision of $\tilde{a}_\mu^{\rm HLO}$ (the analog of $a_\mu^{\rm HLO}$ for our model), i.e., the error obtained from the fit, is much smaller than the accuracy, i.e., the difference between fitted and exact values. We considered correlated fits as well as diagonal fits, and we also considered fits to a science-fiction data set generated with the same covariance matrix scaled by a factor $1/10000$.

From these tests, we conclude that fits based on the VMD-type fit functions we considered cannot be trusted. In nearly all cases, the accuracy is much worse than the precision, and there is no improvement with the more precise data set with the rescaled covariance matrix. Adding parameters (VMD +) does not appear to help. Based on our tests, we therefore call into question the use of VMD-type fits for the accurate computation of $a_\mu^{\rm HLO}$.[12]

The sequence of PAs considered here performs better, if one goes to high enough order. The order needed may be higher if one uses more precise data, as shown in the comparison between Tables I and II. Still, with the lattice Q^2 values and covariance matrix of Ref. [9], the maximum accuracy obtained is of order a few percent, but at least this is reflected in the errors obtained from the fits. Of course, given a certain data set, one cannot add too many parameters to the fit, and indeed we find that adding parameters beyond the [2, 2] PA ([2, 3] PA for the science-fiction data set) does not help: parameters for the added poles at larger Q^2 have such large fitting errors that they do not add any information. We also found that PA fits do less well when one increases the fitting interval, and proposed that the contribution to $a_\mu^{\rm HLO}$ from the region between around 1 GeV^2 and the value where QCD perturbation theory becomes reliable can, instead, be accurately computed using (for instance) the trapezoidal rule (cf. Sec. V D).

The ability of a direct numerical integration of the fake data to accurately reproduce the underlying model contribution in the region above $Q^2 \sim 1$ GeV^2 represents an important observation for the future. The source of the systematic problem for the various fits discussed here is the dominance of these fits by the large range of higher-Q^2 data in the fit windows employed. These data have smaller errors, but tend to lead to a fitted polarization function with less curvature than the true polarization function in the low-Q^2 region which dominates the a_μ integral. Because this low-Q^2 region lies outside the range of presently available data, the size of the resulting systematic error is thus likely to increase as one increases the upper bound of the fit window employed. This expectation is confirmed by the comparison between the results obtained using the larger $0 \le Q^2 \le 1.5$ GeV^2 and smaller $0 \le Q^2 \le 1$ GeV^2 fit windows. One thus wants to optimize the fits by keeping the upper bound of the fit window as small as possible while at the same time retaining sufficient data points to allow fits using PAs of sufficiently high order to produce good representations of the low-Q^2 curvature.

We believe that tests such as that proposed in this article should be carried out for all high-precision computations of $a_\mu^{\rm HLO}$. We have clearly demonstrated that a good χ^2 value may *not* be sufficient to conclude that a given fit is good enough to compute $a_\mu^{\rm HLO}$ with a reliable error. The reason is the "magnifying effect" produced by the multiplication of the subtracted vacuum polarization by the kinematic weight in the integral yielding $a_\mu^{\rm HLO}$. While other useful models [for instance, based on $\sigma(e^+e^- \to \text{hadrons})$ data] may also be constructed, the model considered here, for the $I = 1$ polarization function $\Pi(Q^2)$, is already available, and data on this model will be provided on request.

ACKNOWLEDGMENTS

We would like to thank Christopher Aubin and Tom Blum for discussions. K. M. thanks the Department of Physics at the Universitat Autònoma de Barcelona for hospitality. This work was supported in part by the U.S. Department of Energy, the Spanish Ministerio de Educación, Cultura y Deporte, under program SAB2011-0074 (M. G.), the Natural Sciences and Engineering Research Council of Canada (K. M.), and by CICYTFEDER-FPA2011-25948, SGR2009-894, the Spanish Consolider-Ingenio 2010 Program CPAN (CSD2007-00042) (S. P.).

[12]This includes the recent work in Ref. [24], in which the error on $a_\mu^{\rm HLO}$ is obtained from a VMD+ fit, and in which, reportedly, the error from PA-type fits is much larger. Based on the results we have obtained, we strongly suspect that the error on $a_\mu^{\rm HLO}$ in Ref. [24] is significantly underestimated. For example, the results from the [1,2] PA and VMD+ fits on the interval $0 < Q^2 \le 1.5$ GeV^2 in Table I are compatible within errors, with the PA error five times larger than the VMD+ error. Moreover, in both cases the fit error is too small.

[1] For a recent review, see T. Blum, M. Hayakawa, and T. Izubuchi, Proc. Sci., LATTICE (2012) 022.
[2] T. Blum, Phys. Rev. Lett. **91**, 052001 (2003).
[3] B. E. Lautrup, A. Peterman, and E. de Rafael, Phys. Rep. **3**, 193 (1972).
[4] M. Della Morte, B. Jäger, A. Jüttner, and H. Wittig, J. High Energy Phys. 03 (2012) 055; Proc. Sci., LATTICE (2012) 175.
[5] C. Aubin, T. Blum, M. Golterman, and S. Peris, Phys. Rev. D **88**, 074505 (2013).
[6] C. Aubin and T. Blum, Phys. Rev. D **75**, 114502 (2007).
[7] X. Feng, K. Jansen, M. Petschlies, and D. B. Renner, Phys. Rev. Lett. **107**, 081802 (2011); X. Feng, G. Hotzel, K. Jansen, M. Petschlies, and D. B. Renner, Proc. Sci., LATTICE (2012) 174.
[8] P. Boyle, L. Del Debbio, E. Kerrane, and J. Zanotti, Phys. Rev. D **85**, 074504 (2012).
[9] C. Aubin, T. Blum, M. Golterman, and S. Peris, Phys. Rev. D **86**, 054509 (2012).
[10] A. Francis, B. Jäger, H. B. Meyer, and H. Wittig, Phys. Rev. D **88**, 054502 (2013).
[11] D. Boito, O. Catá, M. Golterman, M. Jamin, K. Maltman, J. Osborne, and S. Peris, Phys. Rev. D **84**, 113006 (2011).
[12] D. Boito, M. Golterman, M. Jamin, A. Mahdavi, K. Maltman, J. Osborne, and S. Peris, Phys. Rev. D **85**, 093015 (2012).
[13] K. Ackerstaff *et al.* (OPAL Collaboration), Eur. Phys. J. C **7**, 571 (1999).
[14] C. Bouchiat and L. Michel, J. Phys. Radium **22**, 121 (1961).
[15] M. Davier, A. Hoecker, G. L. Castro, B. Malaescu, X. H. Mo, G. T. Sánchez, P. Wang, C. Z. Yuan, and Z. Zhang, Eur. Phys. J. C **66**, 127 (2010).
[16] C. E. Wolfe and K. Maltman, Phys. Rev. D **83**, 077301 (2011).
[17] R. R. Akhmetshin *et al.* (CMD-2 Collaboration), Phys. Lett. B **648**, 28 (2007).
[18] M. N. Achasov, K. I. Beloborodov, A. V. Berdyugin, A. G. Bogdanchikov, A. V. Bozhenok, A. D. Bukin, D. A. Bukin, T. V. Dimova *et al.*, Zh. Eksp. Teor. Fiz. **130**, 437 (2006) [J. Exp. Theor. Phys. **103**, 380 (2006)].
[19] J. P. Lees *et al.* (*BABAR* Collaboration), Phys. Rev. D **86**, 032013 (2012).
[20] D. Babusci *et al.* (KLOE Collaboration), Phys. Lett. B **720**, 336 (2013).
[21] P. A. Baikov, K. G. Chetyrkin, and J. H. Kühn, Phys. Rev. Lett. **101**, 012002 (2008).
[22] G. M. de Divitiis, R. Petronzio, and N. Tantalo, Phys. Lett. B **718**, 589 (2012).
[23] X. Feng, S. Hashimoto, G. Hotzel, K. Jansen, M. Petschlies, and D. B. Renner, Phys. Rev. D **88**, 034505 (2013).
[24] F. Burger, X. Feng, G. Hotzel, K. Jansen, M. Petschlies, and D. B. Renner, arXiv:1308.4327.